UNIVERSITÀ DEGLI STUDI DI PALERMO
Ph.D. in Experimental Oncology and Surgery
Department of Surgical, Oncological and Oral Sciences (Di.Chir.On.S.)

Circulating cell-free DNA (cfDNA) and extracellular vesicles (EVs) as prognostic and predictive biomarkers in patients with advanced Non-Small Cell Lung Cancer (NSCLC): the LEXOVE prospective study

Doctoral Dissertation of:
Dott. Valerio Gristina

Tutor:
Prof. Antonio Russo

Years 2019/2022 – Cycle XXXIV

INDEX

Abstract

Despite the increasing implementation of targeted and immune-based treatments, the prognosis of patients with advanced non-small cell lung cancer (NSCLC) remains dismal. Namely, the quantification of cell-free DNA (cfDNA) or extracellular vesicles (EVs) content might be significant for cancer prognostication and response assessment. The LEXOVE trial is a prospective cohort study including the monitoring of treatment-induced changes in the blood profile in treatment-naive advanced NSCLC patients. Agreement between cfDNA/EV dynamics and radiographic tumor response was evaluated in patients with available plasma samples from baseline (T0) to radiologic evaluation (T1). From February 2020 to May 2022, 73 treatment-naïve subjects were consecutively included. A total of 315 liquid biopsy paired samples were collected from 63 patients at baseline and from 47 patients at disease re-evaluation. We further isolated and characterized EVs from plasma samples of 22 patients using an affinity purification method and the Dynamic Light Scattering (DLS) technique. According to the median cfDNA value (0.61 ng/µl) at baseline, the median PFS resulted to be 8.4 (95% CI: 2.5-14.3) and 4.2 (95% CI: 2.5-5.9) months (p=0.043), whereas the OS being 30.3 (95% CI: 18.4-42.1) months and 4.7 (95% CI: 2.6-6.9) months (p<0.0001) in patients with lower and higher cfDNA levels, respectively. Interestingly, a higher value for PFS was observed in the oncogene-addicted cohort (0.92 ng/µl) whereas a lower level for OS was detected in the patients' cohort receiving CT only (0.50 ng/µl). Notably, when assessing the agreement between radiographic and cfDNA response, a fair concordance for 20% cfDNA response (Cohen's kappa coefficient = 0.001) was observed between early and durable radiographic and cfDNA response. Compared to the healthy donor, the number of EVs (R90) resulted to be significantly and steadily higher in patients with advanced NSCLC both at T0 and T1. When assessing the agreement between radiographic and EVs protein content (cfEXO) response, a fine concordance for 20% cfEXO response (Cohen's kappa coefficient = 0.033) was observed between radiographic and cfEXO response. Intriguingly, lower and higher cfDNA levels were matched to lower and higher R90 values in EGFR-positive patients with a partially responding or progressive disease, respectively. Overall, ECOG-PS 2 patients receiving chemotherapy plus pembrolizumab seemed to experience poorer survival in terms of both PFS (p= 0.015) and OS (p=0.036) as compared to single-agent pembrolizumab (p=0.842 and p= 0.644 for PFS and OS, respectively), suggesting a possible predictive value of ECOG-PS in this real-world clinical scenario. In conclusion, this explorative study confirmed the role of cfDNA in real-time longitudinally monitoring while providing a proof of concept for identifying EVs by DLS as early biomarkers in treatment-naïve patients with advanced NSCLC.

CHAPTER 1

Background, rationale and objectives

Lung cancer is the main cause of cancer death worldwide with two million newly diagnosed cases, or 13% of all cancers diagnosed, in 2020.[1] To date, the American Cancer Society's estimates for lung cancer incidence and mortality in the United States are about 236,740 new cases (117,910 in men and 118,830 in women) and 130,818 deaths (68,820 in men and 61,630 in women), respectively.[2] In Italy, it is the second and third most frequently occurring cancer in men (15%) and women (12%), respectively, with 42,500 new estimated cases in 2019 (29,500 in men and 13,000 in women) with still a geographic gradient for tumor incidence from North to South. The Italian Association of Medical Oncology (AIOM) and the Italian Association of Tumor Registries (AIRTUM) estimated moreover about 33,836 deaths from lung cancer in Italy in 2018, with a 5-year survival rate of 16%, influenced by the large proportion of patients with advanced stage, and 10-year survival of 12% (11% for men and 15% for women).

Current histologic classification for lung cancer refers to World Health Organization (WHO) and is recommended before any curative treatment. More than 95% of lung cancers scan be traced back to four main histotypes: squamous carcinoma, adenocarcinoma, large cell carcinoma and small cell lung cancer. In particular, non-small cell lung cancer (NSCLC) accounts for 85–90% of lung cancers including the three main histological subtypes: squamous cell carcinoma (30%), adenocarcinoma (40%), and large cell carcinoma (3–9%).[3]

To date, molecular testing is recommended as part of broad mutational analyses including all these oncogenic driver alterations with the final goal of identifying specific targets for which tailored agents are available in the context of clinical trials. A personalized therapeutic approach based on the detection of activating mutations in the kinase domain of the epidermal growth factor receptor (*EGFR*) and anaplastic lymphoma kinase (*ALK*) rearrangements correlated directly with sensitivity to specific tyrosine kinase inhibitors (TKIs). In addition,

other important driver mutations found in NSCLC included kirsten rat sarcoma virus (*KRAS*), B-Raf proto-oncogene (*BRAF*) and *ERBB2* (*HER2*) mutations, c-ros oncogene 1 (*ROS1*) and *RET* genes rearrangements and *MET* amplifications. So far both first- (erlotinib, gefitinib) and second-generation (afatinib) EGFR TKIs have been the standard first-line treatment options. Unfortunately, almost all patients would eventually develop drug resistance over time through secondary acquired mutations. Accordingly, a third-generation EGFR TKI (osimertinib) has been designed to target the T790M mutation which has resulted to be the most common mechanism of acquired or de novo resistance to TKIs (accounting for approximately 50-60% of pre-treated patients and with a variable frequency in treatment-naive patients) showing improved efficacy in treated and untreated EGFR mutated patients.[4,5] Conversely, other mechanisms of resistance (including *HER-2* and/or *MET* amplification, *PIK3CA* and/or *BRAF* mutation, small cell lung cancer transformation)[6] were revealed to be relatively heterogeneous, only rarely occurring concurrently with T790M mutation and showing a much lower incidence. However, obtaining tissue re-biopsies for molecular analysis has resulted to be challenging in up to 50% of cases either due to patients' comorbidities or insufficient and heterogeneous tumor tissue sampling[7], claiming for the enthusiastic development of minimally invasive methods for molecular testing such as so-called liquid biopsy. Recently, the Food and Drug Administration (FDA) approved the first liquid biopsy companion diagnostic which relies on the molecular analysis of circulating cell-free DNA (cfDNA, released through cell death mechanisms such as necrosis and apoptosis in biofluids) using next-generation sequencing (NGS) technology. In this context, a primary challenge for the detection of circulating tumor DNA (ctDNA), the component of cfDNA released from tumor sites into the blood of cancer patients, has proved to be the low allelic frequencies mutation and low copy numbers of the mutation target. Thus, considering the low abundance and intermediate sensitivity of plasma ctDNA according to specific clinical contexts, a tissue re-biospy is still the gold standard in the case of a ctDNA negative result. Moreover, another paradigm shift in the treatment of NSCLC has been the introduction of immunotherapy with immune checkpoint inhibitors (ICIs) that disrupt co-inhibitory T-cell signalling such as programmed cell death-1 (PD-1) or its ligand PD-L1, showing a clear clinical benefit with increased overall survival (OS) versus standard chemotherapy, both in the second-line setting (nivolumab, pembrolizumab and atezolizumab) and as first-line treatment in PD-L1>50% selected patients (pembrolizumab).[8] Albeit durable responses and improved survival rates have been commonly observed suggesting a long-lasting immunologic memory in large subsets of patients treated with ICIs, some patients would experience primary or secondary immune escape which has not been comprehensively

explored and seemed to differ from the traditional static drug resistance of most anticancer therapies.

Despite the increasing implementation of targeted and immune-based treatments, the prognosis of NSCLC patients remains dismal.[2] In the precision oncology era, liquid biopsy has dramatically revolutionized the management of such patients potentially overcoming tissue biopsy limitations while entering the current clinical practice as a valuable diagnostic tool.[9] Namely, the quantification of ctDNA or cfDNA, released from tumor sites into the bloodstream of cancer patients, emerged as a minimally invasive approach to monitor the real-time tumor evolution with the kinetics of plasma ctDNA during standard treatments revealing as an efficacy predictor for NSCLC patients.[10,11] In the era of personalized medicine, emphasis has been recently placed on circulating extracellular vesicles (EVs) for their role in facilitating early detection and diagnosis while improving treatment outcomes. EVs have been defined as double-membrane structures of 20 – 2000 nm consisting of nucleic acids and proteins, released by a wide range of living cell types and found in various bodily fluids, participating in communication between cells and thereby contributing to tumor growth, metastasis, angiogenesis and drug resistance.[12] An important feature of EVs is that nucleic acids in the lumen of these vesicles are protected from nucleases present in plasma and other biofluids by a lipid bilayer membrane, which allows for the isolation of intact and good quality RNA, DNA and proteins. Though not yet implemented as a clinically valid biomarker for the prediction of tumor responses, the peculiar advantages of using dynamic in vivo biomarkers make cfDNA and EVs appealing tools for therapeutic monitoring during anticancer therapies. Hence, additional data validating the role of such biomarkers in predicting and monitoring clinical outcomes in the first line setting of NSCLC are warranted. In this fascinating scenario, although several biomarkers have been described in the literature[13,14,15,16], there remains an unmet need for the discovery of dynamic in vivo biomarkers to refine the clinical management of advanced NSCLC patients, predicting response and prognostics to eventually improve the optimal treatment sequencing while avoiding ineffective therapies and adverse side effects. Accordingly, a growing body of evidence has proved the utility of circulating EVs as minimally invasive biomarkers in different disease settings, even if merely at the preclinical level.[17,18,19,20] In NSCLC patients, albeit the ctDNA analysis remains the gold standard for routine clinical diagnostics, the interrogation of EV content might be complementary for cancer prognostication and response assessment. In this vein, differing methods of EVs isolation and characterization have been set out with the Dynamic Light Scattering (DLS) representing a promising technique for determining the particle size distribution in a colloidal suspension such

as plasma.[21] Making use of the Brownian Motion of suspended particles in a solvent, DLS would enable the analysis of nanoparticles by evaluating the hydrodynamic diameter (Dz) and the Rayleigh scattering (Rex or R90) for the estimation of diameter and the number of vesicles, resepctively.[22]

This explorative prospective study aimed to describe whether serial plasma cfDNA and tumor-derived EVs measurements could longitudinally reflect response and resistance to available standard treatments, investigating the potential of cfDNA and EVs kinetics to predict clinical outcomes in advanced NSCLC patients undergoing first-line systemic treatments. The main objective was to identify specific liquid biopsy data (cfDNA- and EV-based) which could be measured longitudinally to evaluate the potential of predicting clinical outcomes and monitoring the therapeutic outcome while investigating novel potential biomarker dynamics to select patients with advanced NSCLC who are likely to respond to standard treatments. By using biophysics and bioinformatics approaches, this pilot study aimed to elucidate the role of early detection of circulating biomarkers as reliable biomarkers in terms of prognostic/predictive significance in the clinical setting, paving the way for a larger controlled prospective study.

CHAPTER 2

Materials and Methods

2.1 Study design and patients

The LEXOVE trial is a prospective cohort study including the systematic assessment of tumor biopsies at baseline and the monitoring of treatment-induced changes in the blood profile in treatment-naive advanced NSCLC patients who were candidates to receive standard first-line treatments. From February 2020 to May 2022, patients with advanced NSCLC (stage IIIB to IV) treated at the Medical Oncology Unit of Paolo Giaccone University Hospital, Palermo Italy were consecutively enrolled. Tumor tissue was obtained by systematic biopsy at baseline and stored as a formalin-fixed paraffin-embedded (FFPE) sample at the Department "G. D'Alessandro", Pathology Institute, University of Palermo and at other referring Pathology Units. Isolation and characterization protocols along with survival analysis were carried out in patients with advanced NSCLC receiving available standard first-line treatments with available plasma samples. Agreement between cfDNA/EV response and radiographic tumor response was evaluated in patients with available plasma samples from T0 to T1 and at least two clinical follow-ups for therapeutic assessment. All FFPE samples were analyzed in the Laboratory of Molecular Oncology at the “Regional Reference Center for the prevention, diagnosis and treatment of rare heredo-familial cancers of adults Medical Oncology” (Medical Oncology Unit, Department of Surgical, Oncological and Oral Sciences, A.O.U.P. “P. Giaccone” University Hospital of Palermo), an accredited Italian reference genetic center for prognostic and predictive molecular testing in oncology. In collaboration with the Institute of Biophysics

at the Italian National Research Council (CNR), circulating EVs were isolated and characterized by DLS.

Paired whole blood samples (~5 mL) were collected at baseline and at the first radiologic evaluation of disease (within 12 weeks) during the treatment course according to a standardized protocol and stored frozen. All the patients underwent a CT scan every 3 months and radiologic responses were classified according to the Response Evaluation Criteria in Solid Tumors (RECIST) version 1.1. CT scans were collected at baseline and every 3–6 months as per clinical practice.[23] Clinical and pathological characteristics of all NSCLC patients included in our study were retrieved from the clinical records available and were assessed retrospectively. Medical records of patients included in the study were reviewed to collect clinical information, including demographics, baseline clinical features, tumor- and treatment-related data. Only patients with adequate follow-up information, including disease status or death at database lock, and complete clinical records were considered for study analysis. Inclusion criteria included: (1) Eastern Cooperative Oncology Group (ECOG) Performance Status (PS) of ≤ 2; (2) patients with histologically- or cytologically-documented NSCLC with unresectable stage IIIB-C or Stage IV Disease (according to Version 8 of IASCL TNM) who were treatment-naive and eligible for first-line TKIs (osimertinib, alectinib, crizotinib, dabrafenib+trametinib), IO-based treatment (pembrolizumab +/- platinum-based chemotherapy [CT]) or CT only. Exclusion criteria included: (1) patients with other malignant tumors; (2) patients with ECOG PS ≥ 3; (3) patients who received prior first-line TKIs or IO +/- platinum-based chemotherapy; (3) patients with mental illness prohibiting informed consent. The study was approved by the Local Ethical Committee according to the principles outlined in the Declaration of Helsinki. The written informed consent to participate was obtained from all patients that permitted for use of their peripheral blood and clinical records.

2.2 FFPE tissue collection, nucleic acids extraction and molecular analysis

The mutational status was tested on the thickness of 10 μm obtained by biopsy at baseline or resected tumor tissue stored as FFPE samples for the detection of oncogene addiction. PD-L1 immunohistochemistry (IHC) was carried out on 4-μm sections of FFPE tumor tissue samples using Dako PD-L1 IHC 28-8 PharmaDx (Agilent) and evaluated by a trained pathologist according to the tumor proportion score (TPS), defined as the percentage of positive viable tumor cells among all viable tumor cells evaluated.[24]

The FFPE tissue samples were collected from the archive of the Pathology Department

University Hospital of Palermo or other referring Institutions of Pathological Anatomy. DNA and RNA nucleic acids were extracted from six 10 μm thickness FFPE tissue sections with an adequate percentage of neoplastic cells. The genomic DNA and RNA were extracted from FFPE tissue using the QIAmp FFPE Tissue Kit and RNeasy FFPE kit (Qiagen, Hilden, Germany), respectively and quantified in terms of ng/μl using QubitTM dsDNA HS Assay Kit and QubitTM RNA HS Assay Kit (ThermoFisher Scientific, Foster City, CA, USA), respectively. As recommended by the most recent AIOM and ESMO guidelines and according to clinical practice, a few nanograms of DNA and RNA including EGFR, BRAF, KRAS, ALK, ROS1 genes alterations, MET amplification, and eventually the gene fusion transcripts were tested using the OncomineTM Focus DNA/RNA panel. Moreover, the OncomineTM RNA assay offered the opportunity to evaluate the 5'/3'imbalance ratio at the ALK, ROS1, RET and NTRK1 genes as a fusion signature independently by the unknown partner. Libraries were quantified by Ion Library TaqManTM quantification kit on QuantStudio7 Pro Real-Time PCR System (Applied Biosystem) using Design&Analysis Software v2.4.3. The analytical sensibility of the assay achieved at an allelic frequency ≥5% was 100%, but the performance of every single run was referred to the data. The data were tested on an amplicon-based sequencing platform: Ion Torrent S5TM System. The Oncomine Focus-520-w.30-DNA-Single Sample and the Oncomine Focus-520-w.30-Fusions-Single Sample represented the workflow applied for the analysis of DNA and RNA samples. To test the reliability of data for DNA sequencing, we complied with the following thresholds: mapped read >300.000, mean read length >75 bp, uniformity >90%, and mean raw accuracy >99%. Whereas, for RNA sequencing, we considered acceptable an analysis with mapped read >50.000, mean read length >60 bp, and expression controls detected ≥3 out of 5. All reagents, kits and platforms used were ThermoFisher Scientific, Foster City, CA, USA. The data of DNA sequencing were analyzed with Ion Torrent TorrentSuiteTM (TS, version 5.18) processing the plug-in of Coverage Analysis and Variant Caller. Integrative Genomics Viewer (IGV v2.4.1) was used to visibly evaluate the alignments of sequences. Pathogenetic changes in DNA, and RNA sequences with the related percentage of allelic frequency were annotated, only for DNA analysis, by Ion Reporter Software v5.18 applying the filter chains Oncomine variants for default use and DefaultFusion View 5.18, respectively. They were described using the HGVS standard nomenclature. To confirm the data of common pathogenic variants or the cases of poor quality and quantity DNA, 15-30 ng of DNA was amplified using EasyPGX ready EGFR/BRAF/KRAS kit with a LOD of 5%. After about 2h run, the data obtained on Real time EasyPGX System (Diatech Pharmacogenetic, Jesi AN-Italy) were analyzed using EasyPGX

Analysis Software v4.0.10.

2.3 Plasma separation, DNA extraction, cfDNA quantification and molecular analysis

Blood samples (~5 mL) have been collected into K2 EDTA tubes at baseline before the first drug administration and at each instrumental disease re-evaluation during the treatment course. They were immediately processed for plasma collection and centrifuged twice (10 minutes at 3000 rpm; 10 minutes at 16,000 x g). Sample processing was carried out within 2h of the plasma collection. Collected plasma samples have been used to extract cfDNAs as well as to isolate EVs. cfDNAs were extracted from 1 to 2 ml of plasma using QIAamp Circulating Nucleic Acid Kit (Qiagen). cfDNA quantified in terms of ng/µl using QubitTM dsDNA HS Assay Kit. Cell-gree nucleic acids (cfNAs) were performed throughout time using OncomineTM Lung cfTNA Research Assay. Every single NGS run findings were compared with positive in-house control as a validation set. Libraries were quantified by Ion Library TaqManTM quantification kit on QuantStudio7 Pro Real-Time PCR System (Applied Biosystem) using Design&Analysis Software v2.4.3. Using 20 ng of cfNAs, the specificity of this kit was 99% at 0.1% of the limit of detection (LOD). The data were tested on an amplicon-based sequencing platform: Ion Torrent S5TM System. The Oncomine TagSeq Lung v2 Liquid Biopsy-w2.5-Single Sample represented the workflow applied for the analysis of cfNAs samples. To test the reliability of data for cfTNAs sequencing, we complied the following thresholds: total mapped reads >3M, median read coverage Avg 40,000 -Min>25,000, median molecular coverage >2,500. The data of DNA sequencing were analyzed by Ion Torrent TorrentSuiteTM (TS, version 5.18) processing the plug-in of Coverage Analysis and Variant Caller. The sequencing data were categorized by relevance with the related percentage of VAF as annotated by Ion Reporter Software v5.18 applying the filter chains Variant Matrix Summary (5.18) for default use.

2.4 EVs isolation and characterization

Following the minimal experimental requirements for isolating and characterizing EVs according to the 2018 position statement of the International Society for Extracellular Vesicles, we isolated EVs from 2 ml of plasma using exoEasy Maxi Kit (Qiagen, USA), a membrane affinity purification method based on commercial EV isolation kits, according to the manufacturer's protocol. EV protein content (cfEXO) was determined by the Bradford assay. In brief, 10 µl of EVs resuspended in PBS were added to 200 µl of Coomassie Protein Assay

Reagent (Pierce, Rockford, IL, USA). The absorbance at 595 nm, was measured with the spectrophotometer (SPECTROstar nano BMG LABtech). The protein concentration was calculated using a standard curve of a dilution series of bovine serum albumin (BSA) whose concentrations are known. Moreover, an aliquot of the isolated EVs, eluted in buffer XE, was pipetted, centrifuged at 1000 g for 10 minutes at 4 °C to remove any dust particles, poured directly into a quartz cuvette and put at 20 °C in a thermostated cell compartment of a BI200-SM goniometer (Brookhaven Instruments) equipped with a He-Ne laser (JDS Uniphase 1136P) at 633 nm and a single pixel photon counting module (Hamamatsu C11202-050). The scattered light intensity and its time autocorrelation function g2(t) were measured simultaneously at 90° (R90) by using a BI-9000 correlator (Brookhaven Instruments). Absolute values for scattered intensity (excess Rayleigh ratio, Rex or R90) were obtained by normalization with respect to toluene and subtraction of the buffer signal.[25] The excess Rayleigh ratio or R90 is proportional to the particle number concentration N, the squared weight-averaged mass (Mw)2, and to the form factor P(q); therefore, in the case of particles with the same size and shape, it can be taken as rough esteem of the vesicle amount. The autocorrelation functions were fitted by a two-component Schultz distribution for the diffusion coefficient D.[26,27] Then, the intensity-weighted distribution of hydrodynamic radii Dh is determined by using the Stokes–Einstein relation $D = (kBT)/(3\pi\eta Dh)$, where kB is the Boltzmann constant, T is the temperature, and η is the medium viscosity, that is assumed to be the same as PBS. Indeed, a dynamic light scattering measurement was performed both on a vesicle sample in buffer XE and on the same sample in PBS. This buffer exchange was performed by HPLC-SEC run on a Sepharose CL-2B column by recovering the void volume fraction to eliminate the small size particles due to buffer XE. The first component of the distribution (not shown) amounts to less than 5% of the signal and refers to small size particles (less than 20 nm) present in the samples. By considering the second component of the distribution, which is related to vesicles, one measures the average and the normalized variance, corresponding to the z-averaged hydrodynamic diameter (Dz) and the polydispersity index (PDI) of vesicle distribution, respectively.[28]

2.5 Statistical Analysis

Descriptive statistics were used to analyze demographic and clinical data. For the cfDNA and EVs kinetic analysis, consecutive paired blood collection was performed at baseline and the radiological response assessment within 12 weeks of the serial follow-up. According to radiologic response, efficacy was defined as responsive (complete response [CR] or partial response [PR]) or non-responsive disease (stable disease [SD] or progressive disease [PD]),

based on the standard RECIST 1.1. Regarding cfDNA, we dichotomized values as ≥ and < 20% indicating the change from baseline cfDNA to higher and lower levels, respectively, after the initiation of treatment. We used X-tile analysis to determine the optimal cfDNA cut-off value for survival prediction, according to PFS and OS. A paired Wilcoxon test was used to compare the median cfDNA plasma levels at baseline and according to the radiologic response evaluation. Cohen's kappa test was used to determine the concordance of dynamic changes in liquid biopsy data and radiologic response with a 95% confidence interval. Pearson chi-square or Fisher's exact test was used to determining any statistically significant association between cfDNA or EVs dynamics and radiologic response to systemic treatments.

The Kaplan–Meier method was used for performing survival analysis, providing median and p values, with the use of the log-rank test for comparisons. Univariate and multivariate analyses were performed using the Cox proportional hazards and logistic regression models. The multivariable model included as covariates all pretreatment parameters found to have a p-value <0.05 at univariate analysis.

Progression-free survival (PFS) was calculated from the date of study inclusion to the first evidence of disease progression or death from any cause or censored at the most recent follow-up. Overall survival (OS) was defined from the date of study inclusion to death from any cause or censored at the most recent follow-up. A p-value < 0.05 was used as the threshold for statistical significance. All the statistical analyses were performed using SPSS statistics software, version 20 (IBM, Armonk, NY, USA).

CHAPTER 3

Results

3.1 Pathological and demographic characteristics

From February 2020 to May 2022, a total of 87 patients were screened for eligibility and met the inclusion criteria. Among these, 73 treatment-naïve subjects with adequate follow-up information and complete clinical records were considered for study analysis and were finally included in the study. The clinical characteristics of the patients enrolled in this study are shown in Table 1. Most patients were aged over 65 years old (54.8%), male (71.2%), current or former smokers (76.7%) while presenting with adenocarcinoma histology (76.7%) and an ECOG-PS of 0-1 (57.5%). Notably, a significant portion (42.5%) of the included patients exhibited an ECOG-PS 2. The largest part of the cohort population presented with a locoregional lymph node involvement (84.9%) with the most common distant metastatic sites being represented by bone (32.8%), followed by the central nervous system (CNS; 19.2%), adrenal gland (17.8%) and liver (12.3%).

As far as tissue diagnostics is concerned, all non-squamous tumors were tested. Among these, 55 (75.3%) samples were assessed for *EGFR* or *BRAF* mutations using RT-PCR with the total mutation rate being 20% (11/55), detecting eight and three hotspot point mutations, respectively. On the other hand, even if only 9 (12.3%) tissue specimens were evaluated, the total mutation rate using DNA/RNA-based NGS was 66% (6/9), covering nine different activating genomic alterations within *EGFR*, *KRAS*, *ALK*, *MET*, *RET* and *ROS1* genes. As regards IHC, 67 (91,7%), 56 (76,7%) and 46 (63,0%) samples were tested for PD-L1, ALK and ROS1. Finally, only 5 (6.8%) patients underwent plasma genotyping via NGS. Table 2 comprehensively summarizes all the diagnostic techniques performed during the conduction of this study.

All the 73 included patients received systemic treatments in the front-line setting. Namely, 19, 28 and 26 patients received treatment based on TKI, IO and CT, respectively. At the time of survival analysis (median follow-up of 20.73 months, range: 17.36-24.1 months), 51 patients had disease progression, while 42 patients died because of tumor progression with 31 patients being still alive at the time of data analysis. Median PFS and OS resulted to be 6.1 (95% CI: 4.0-8.2) and 12.8 (95% CI: 2.1-23.5) months in the overall population, respectively. Among specific treatment subgroups, median PFS and OS were 6.0 (95% CI: 0-25.5) and 32.6 (95% CI: 0-72.7) months, 10.3 (95% CI: 0-24.3) and 20.5 (95% CI: 6.9-34.1) months, and 4.2 (95% CI:2.5-5.9) and 9.0 (95% CI: 6.3-11.6) months in patients receiving TKI, IO and CT, respectively (Figure 1). Namely, when compared to CT only, patients receiving TKIs or IO-based treatments were confirmed to experience significantly improved PFS (p=0.022 and p=0.006, respectively) and OS (p=0.054 and p=0.057, respectively).

Briefly, a total of 315 liquid biopsy samples were collected from 63 patients at baseline with a total of paired plasma samples from 47 patients at disease re-evaluation. Among 63 patients evaluable for cfDNA analysis at baseline, the median cfDNA level was 0.61 ng/µl, thus not significantly higher than that observed in 47 patients evaluated at the first follow-up point within twelve weeks during the treatment course (0.57 ng/µl, Wilcoxon rank-sum test p = 0.536). Here we report the graphical representation of the results of the longitudinal monitoring by cfDNA at T0-T1 from 63 patients in our study cohort (Figure 2).

3.2 Prognostic and predictive value of cfDNA levels at baseline

Firstly, to better evaluate the predictive role of baseline cfDNA levels, we divided the overall cohort population into cfDNA-low and -high groups by the median cfDNA value (0.61 ng/µl). Accordingly, the median PFS resulted to be 8.4 (95% CI: 2.5-14.3) and 4.2 (95% CI: 2.5-5.9) months (p=0.043), whereas the OS was 30.3 (95% CI: 18.4-42.1) months and 4.7 (95% CI: 2.6-6.9) months (p<0.0001) in patients with lower and higher cfDNA levels, respectively (Figure 3).

To enhance the prediction accuracy, we sought to reliably evaluate the utility of baseline cfDNA levels as a predictive tool for the overall population and according to treatment subgroups, dichotomizing patients into two groups (cfDNA-low and -high) according to a refined threshold calculated based on the X-tile analysis. In the all-comers population, a baseline cfDNA cut-off value of 0.68 ng/µl both for PFS and for OS seemed to reliably discriminate between patients with good and poor prognosis (Figure 4). Accordingly, the

median PFS was 8.3 (95% CI: 3.3-13.4) months in the baseline cfDNA-low group and 4.5 (95% CI: 3.2-5.8) months in the baseline cfDNA-high group (p=0.038), whereas the median OS was 23.3 (95% CI: 9.7-36.9) and 4.5 (95% CI: 3.4-5.5) months in the two cfDNA categories (low vs. high baseline levels, respectively; p<0.0001) (Figure 4).

In the oncogene-addicted disease, we observed a baseline cfDNA cut-off value of 0.92 ng/µl for PFS (median PFS = 24.0 months, 95% CI: 0-48.6 months in the cfDNA-low group versus median PFS = 2.5 months, 95% CI: 0-5.1 months in the cfDNA-high group), even if not reaching the statistical significance (p=0.293); on the other hand, patients receiving TKIs with cfDNA concentrations higher than 0.68 ng/µl had significantly shorter OS (median OS= 4.0 months, 95% CI: 2.9-5.0 months) than those with lower cfDNA concentrations (median OS= 32.6 months, 95% CI: 0-76.5 months) (p=0.044) (figure 5).

Dealing with the IO subgroup, patients presenting with baseline cfDNA level higher than 0.65 ng/µl seemed to experience poorer PFS (median PFS = 6.1 months, 95% CI: 0-14.0 months) and OS (median OS = 6.1 months, 95% CI: 0.1-12.0 months) when compared to patients with lower cfDNA concentrations (median PFS and OS = not reached [NR]) (p= 0.021 and 0.012, respectively) (Figure 6).

As far as the CT subgroup is concerned, patients with baseline cfDNA levels higher than 0.63 ng/µl and 0.50 ng/µl showed a significantly shorter PFS (median PFS = 3.9 months; 95% CI: 0.4-7.3 months) and OS (median OS = 5.7 months; 95% CI: 3.5-7.9 months) than those with lower cfDNA concentrations (median PFS = 6.8 months; 95% CI: 6.1-7.4 months; median OS = 20.2 months; 95% CI: 14.7-25.7 months) (p= 0.022 and 0.018, respectively) (Figure 7).

3.3 Dynamic plasma cfDNA values are associated with radiologic response and survival outcomes

During this study, 47 out of 63 patients with available paired cfDNA values after 12 weeks of systemic treatment were monitored and assessed according to the radiologic evaluation and survival outcomes. We compared baseline and post-treatment cfDNA levels between responders (complete or partial response, N = 23) and non-responders (stable or progressive disease, N = 24). A 20% median cfDNA increase was detected and used as the cut-off point for survival analysis.

While 16/20 (80%) patients presenting with at least a 20% increase did not experience a disease response at first restaging, 19/27 (70.4%) subjects with a sharp drop in the cfDNA level showed a prompt response to systemic treatments (Pearson chi-square test = 11.665). Strikingly, the response ratio of cfDNA responders (19/27, 70.4%) resulted 3.7-fold higher than that of cfDNA

non-responders (4/20, 20.0%). Notably, when assessing the agreement between radiographic and cfDNA response from T0 to T1, a fair concordance for 20% cfDNA response (Cohen's kappa coefficient = 0.001) was observed between early and durable radiographic and cfDNA response.

Since the cfDNA dynamic change during treatment strongly correlated with the response evaluation, data from patients stratified by therapy regimens were further analyzed. Notably, 11 and 18 patients receiving molecularly targeted (Pearson chi-square test = 4.278; Cohen's kappa coefficient = 0.039) and IO-based (Pearson chi-square test = 7.481; Cohen's kappa coefficient = 0.006) therapeutic approaches showed a significant correlation between dynamic cfDNA levels and first radiologic evaluation, respectively, whereas among 18 patients undergoing CT a significant correlation was not observed (Pearson chi-square test = 0.720; Cohen's kappa coefficient = 0.396).

In this vein, we strived to associate cfDNA dynamics with survival outcomes to provide further clinical insights. Overall, within the cfDNA responsive group, 27/47 (57%) patients had a significantly improved median PFS (18.9 months; 95% CI: 6.2-31.5) when compared to 20/47 (43%) cfDNA non-responders (3.3 months; 95% CI: 2.9-3.8) (p=0.004) (Figure 8). Contrariwise, no benefit in terms of OS was observed (30.3 months, 95% CI: 12.2-48.3 vs 20.5 months, 95% CI: 14.4-26.6, respectively; p=0.133) (Figure 8). Considering the PFS results, we stratified survival data according to treatment subgroups. When compared to cfDNA non-responders, cfDNA responsive patients receiving TKI and IO experienced numerically longer PFS (24.0 months [95% CI: 0-52.3] vs 2.5 months [95% CI: 0-18.3], and NR vs 3.4 months [95% CI: 0-19.6], respectively), although not showing any statistical significance (p=0.219 and 0.338, respectively). On the other hand, dealing with cfDNA responders undergoing CT, we noticed significantly improved survival in terms of both clinical and statistical relevance (7.6 months [95% CI: 5.0-10.2] vs 3.2 months [95% CI: 1.5-4.9], p=0.025).

3.4 Survival outcomes and multivariate analysis

Multivariable Cox proportional regression analyses were performed to assess whether a cfDNA increase over the first 12 weeks of therapy represented an independent factor related to the effectiveness of systemic treatments in terms of PFS and OS. All pretreatment variables presenting with a p-value <0.05 at univariate analysis were included as covariates in the multivariable model.

Multivariable analysis identified the presence of liver metastasis (hazard ratio [HR]: 0.027; 95% confidence interval [CI], 0.004-0.175; p = <0,0001) and a cfDNA increase >20% (HR:

0.345; 95% CI, 0.165 - 0.722; p = 0.005) as factors significantly associated with worse PFS (Table 3). Interestingly, as regards OS, multivariable analysis confirmed the occurrence of liver metastasis [HR 0.314, CI 0.14-0.697, p=0.004] as a variable associated with worse survival while further revealing ECOG PS 0-1 and a lower median cfDNA as independent prognostic factors for OS. Accordingly, an ECOG-PS of 0 was associated with a significantly reduced risk of death (HR 0.22, CI 0.08-0.614, p=0.004), compared with ECOG-PS 2 (Table 4).

3.5 The predictive role of ECOG-PS

Considering the multivariable analyses, the role of ECOG-PS in the overall cohort population was further explored according to the available matched cfDNA samples. Overall, compared to patients with ECOG-PS scores of 0 or 1, those patients with ECOG-PS of 2 seemed to experience significantly poorer median PFS (4.2 [95% CI 2.3-6.1] vs 8.3 [95% CI 3.5-13.1] months; p=0.024) and OS (6.1 [95% CI 2.5-9.7] vs 23.3 [95% CI 12.0-34.6] months; p= <0.0001).

Stratifying data by treatment subgroups when comparing to ECOG-PS 0-1 patients, the median PFS resulted to be numerically lower in ECOG-PS 2 patients undergoing TKIs, even if not formally reaching the statistical significance (4.0 [95% CI 0-8.3] months vs 24.0 [95% CI 0-57.4]; p=0.123). Similarly, patients with poorer PS receiving IO-based treatments had a numerically lower median PFS while showing a significant trend for statistical significance (6.1 [95% CI 0.6-11.5] months vs NR; p=0.088). Contrariwise, no statistically significant differences in terms of PFS between ECOG-PS 2 and 0-1 patients undergoing only CT regimens were observed (3.2 [95% CI 2.1-4.3] months vs 6.5 [95% CI 1.5-11.4]; p=0.354).

On the other hand, as far as median OS is concerned, patients with ECOG-PS 2 receiving TKIs or CT had clinically and statistically poorer survival (4.0 [95% CI 3.2-4.8] months vs 32.6 [95% CI NR-NR], p=0.003; 4.8 [95% CI 0-9.9] months vs 18.5 [95% CI 1.9-35.0], p=0.039, respectively). Likewise, even if only showing a strong trend for the formal statistical significance, those patients with poorer clinical conditions undergoing IO-based treatments exhibited poorer survival when compared to ECOG-PS 0-1 patients (12.1 [95% CI 3.9-20.4] months vs NR, p=0.074). Intriguingly, when singly comparing patients receiving pembrolizumab in association or not with chemotherapy within the IO-based subgroup, ECOG-PS 2 patients receiving the combination approach seemed to experience poorer survival in terms of both PFS (p= 0.015) and OS (p=0.036) (Figure 9) as compared to single-agent pembrolizumab (p=0.842 and p= 0.644 for PFS and OS, respectively), suggesting a possible predictive value of ECOG-PS in such patients.

Finally, among 26/63 (41.2%) and 37/63 (58.8%) patients presenting with ECOG-PS 2 and 0-1 evaluable for cfDNA kinetics, no significant association nor correlation between early cfDNA and the radiologic response was observed (Pearson chi-square test = 0.003; Cohen's kappa coefficient = 0.959). However, in patients presenting with poorer clinical conditions, we noticed that mean baseline cfDNA levels were 2.6-fold higher than in patients with an ECOG-PS of 0-1 (1.71 vs 0.65 ng/µl; p=0.105).

3.6 EVs isolation, characterization and dynamics

Briefly, we isolated EVs from plasma samples of 22 patients using an affinity purification method based on commercial EV isolation kits. We checked for size and concentration by implementing DLS that evaluated the integrity and purity of EVs, taking into consideration Dz and R90 (or Rex) for the estimation of diameter and the number of vesicles, respectively, together with the PDI value. In addition, DLS and cfDNA analyses were performed on a healthy volunteer at T0 and T1 to highlight any significant differences as compared to healthy control. Finally, the amount of EVs proteins (named as cfEXO), calculated by the Bradford Assay, was recovered to investigate the mean protein content per vesicle.

Among 22 consecutive patients with sufficient biospecimens evaluable for cfDNA and EV analysis, Bradford and DLS analyses were carried out in 17 and 16 patients at baseline, and in 17 and 13 at the first follow-up point during the treatment course with a total of 12 and 13 paired samples being evaluable for EVs kinetics, respectively.

Compared to the healthy donor, R90 values resulted to be significantly and steadily higher in patients with advanced NSCLC both at T0 and T1, whereas no substantial differences in Dz and PDI were observed (Table 5). Thus, to discover EV-based biomarkers, we evaluated the dynamics of cfEXO and R90 in the overall cohort population. Accordingly, as previously done for the evaluation of cfDNA dynamics, we compared baseline and post-treatment levels between responders and non-responders, detecting a 20% median increase of both cfEXO and R90 as the cut-off point for analyses. While the entirety of patients presenting with at least a 20% cfEXO increase (7/7, 100%) did not experience a disease response at first restaging, 3/6 (50%) subjects with a sharp drop in the cfEXO level showed a prompt response to systemic treatments, trending to the proper statistical significance (Fisher's exact test = 0.07) with a slightly improved survival benefit (median PFS = NR vs 6.8 [95% CI 0-13.8] months, respectively, p=0.116; median OS = NR vs NR, p=0.361) and a 2-fold higher response ratio

among cfEXO responders when compared to cfEXO non-responders, respectively (Figure 10). Remarkably, when assessing the agreement between radiographic and cfEXO response from T0 to T1, a fine concordance for 20% cfEXO response (Cohen's kappa coefficient = 0.033) was observed between early and durable radiographic and cfEXO response.

Conversely, as regards R90 dynamics, no statistically significant differences in terms of median PFS (p=0.354), median OS (p=0.492), association (Fisher's exact test = 1.00), or concordance with the radiologic response (Cohen's kappa coefficient = 0.715) between responders and non-responders were observed. However, according to the available plasma samples from T0 to T1, when comparing *EGFR*-mutated patients receiving TKIs with patients undergoing IO-based or CT regimens, a sharp drop or increase in the R90 level was promptly associated with a radiographic response or progression, respectively (Table 5). Noteworthy, one patient (LEXOVE32), initially diagnosed with an ALK-positive disease by IHC, showed a clear R90 decreasing level, although progressing on alectinib at the first restaging. Finally, this patient resulted to display an *EGFR* activating mutation (p.E746_A750del) without any *ALK* alterations on the plasma NGS profiling, suggesting a possible correlation between TKI activity and number reduction of vesicles while further confirming the improved accuracy of multiplexing analysis compared to IHC in the diagnostic setting of NSCLC.

3.7 Longitudinal monitoring by liquid biopsy data

Finally, focusing on patients with sufficient biospecimens for cfDNA/EV analysis and at least two clinical follow-ups for therapeutic assessment, here we report the graphical representation of the results of the longitudinal monitoring by liquid biopsy (cfDNA, cfEXO and R90) (Figure 11).

CHAPTER 4

Discussion

Over the last decades, liquid biopsy has been playing a key role in the large and rapidly evolving landscape of medical oncology, resulting in a powerful and cost-effective biomarker with the potential to improve survival prediction and outcomes in the NSCLC setting.[29] Even if emerging as a useful method for real-time monitoring of the efficacy of targeted therapies, however, the evaluation of circulating biomarkers for the efficacy of CT or IO combinations has been widely controversial.[30,31] Nonetheless, several research groups have recently suggested the increasing role of cfDNA as a valid tool for the longitudinal monitoring of patients receiving immunotherapy, although being crucially limited by the variable heterogeneity of patients and methodologies.[32,33] In this fascinating scenario, further unbiased real-world clinical studies evaluating the putative role of liquid biopsy in the early distinction between responders versus non-responders to new treatments are warranted before a broad implementation in clinical practice.

We designed a prospective biomarker trial to evaluate the prognostic value of cfDNA and the association of cfDNA dynamic changes with the radiographic response and clinical outcomes in treatment-naïve patients with advanced NSCLC in the real-life setting. In our study, the patients were eligible for receiving first-line standard systemic treatments as per clinical practice and underwent plasma collection at baseline and at the time of first radiologic evaluation. According to specific treatment subgroups, the median survival and the clinical-pathological characteristics seemed to mirror those observed in larger phase III trials.[5,34,35] Hence, this would suggest a real-world clinical scenario providing real-world evidence while entirely representing the actual clinical practice population without compromising the generalizability to the general population of the highly selective randomized clinical trials. Accordingly, patients undergoing TKIs or IO-based treatments seemed to experience significantly improved median survival compared to patients receiving CT only. Withal,

patients presenting with liver disease, ECOG-PS 2 and a cfDNA increase at first restaging were associated with worse survival outcomes. Remarkably, our findings from this real word evidence study were consistent with previously published data, although considering that patients with poorer clinical conditions tended to be excluded from randomized clinical trials[36] while other reports did not prove the straight correlation between cfDNA dynamics and the radiological response.[37] In this vein, with phase III trials on immunotherapy not enrolling patients with ECOG-PS 2 whereas clinical trials on TKIs only including a small proportion of such patients, the negative prognostic outcome of ECOG-PS 2 has been confirmed in only a few retrospective studies including patients with poor clinical conditions undergoing a combination approach based on chemotherapy plus immunotherapy.[38,39] Hence, although similar data have been reported, our data included novel and relevant aspects such as the putative predictive role of ECOG-PS 2 and cfDNA/EV dynamics in this real-world NSCLC prospective clinical study.

In this study, FFPE tissue and plasma samples represented the biological materials used to investigate the potential genetic alterations as a snapshot of the solid and circulating tumor at different time points. Consistent with other studies ref, among both the all-comers population and the specific treatment subgroups, patients with higher baseline cfDNA levels showed significantly shorter median survival than those with low cfDNA concentrations, further validating the prognostic value of cfDNA at baseline. Accordingly, it is well known that patients presenting with a high tumor burden may be associated with high cfDNA levels, thus correlating cfDNA shedding with poor survival outcomes. Although the prognostic role is well established, the clinical ability of cfDNA in predicting efficacy in the upcoming real-world setting of NSCLC remains far from clear. Namely, considering the possible risk of bias using only median or quartiles, we implemented the automatic X-tile software to optimally define cut-off threshold cfDNA values that reliably discriminated patients who would benefit from first-line systemic treatments. Interestingly, as compared to the median value (0.61 ng/µl), a higher value for PFS was observed in the oncogene-addicted cohort (0.92 ng/µl) whereas a lower level for OS was detected in the patients' cohort receiving CT only (0.50 ng/µl).

We then investigated whether cfDNA clearance or a certain degree of cfDNA reduction reflected by cfDNA 20% drop at T1 would better correlate with radiologic response and survival. Overall, early changes in cfDNA during first-line standard treatments seemed to predict the later radiologic response with a median 20% cfDNA increase at the first restaging being significantly associated with a radiologic progression of the disease. While not being

statistically significant for those patients receiving CT only, these findings were consistent in patients undergoing TKIs or IO-based treatments, thus validating the predictive role of cfDNA dynamics in these specific subsets of patients with advanced NSCLC. Likewise, although considering the immature follow-up, all the cfDNA responders seemed to benefit the most in terms of PFS, while not showing any trending advantage in terms of OS which is probably influenced by later line treatments.

Furthermore, we successfully isolated and characterized EVs by DLS at different timepoints in patients with advanced NSCLC undergoing front-line treatments, identifying dramatically higher R90 and cfEXO values both at T0 and T1 when compared to healthy control. Thus, this would suggest a possible role of circulating EVs in terms of prognostic or predictive significance in the advanced NSCLC setting. Dealing with EVs dynamics, a median 20% increase of cfEXO at the first restaging was significantly concordant with a radiologic progression of disease whereas no differences in terms of R90 levels change were observed. Intriguingly, lower and higher cfDNA levels were matched to lower and higher R90 values in EGFR-positive patients with a partially responding or progressive disease, respectively, as opposed to other patients treated with IO-based or CT regimens. Accordingly, in the EGFR-positive population undergoing TKIs, the R90 parameter reflecting the number of EVs seemed to follow the standard instrumental disease re-evaluation according to RECIST 1.1 criteria. On the other hand, the Dz parameter reflecting the diameter of EVs did not seem to be a reliable biomarker, probably influenced by the interactions within the dispersion plasma.

Limitations of the study included the heterogeneity of clinical-pathological characteristics (however reflecting a real-world clinical scenario), the smaller number of patients undergoing EVs evaluation, and the immature follow-up which may have underestimated the final overall results and survival analyses.

In conclusion, this hypothesis-generating study confirmed the role of cfDNA in real-time longitudinally monitoring while providing a proof of concept for identifying EVs characterized by DLS as early biomarkers in terms of prognostic and/or predictive significance in treatment-naïve patients with advanced NSCLC. In this complex and fascinating scenario, this study contributed to the early detection of patients who have experienced drug resistance to first-line treatments favoring the identification of potential prognostic and/or predictive biomarkers which may help future research efforts to select patients for new treatment strategies in the context of larger prospective studies. These preliminary results could favor the selection of new therapeutic targets to be addressed in basic research and clinic trials, advising the preclinical

research professionals and the academic circle on new prognostic and/or therapeutic biomarkers.

CHAPTER 5

Figures and tables

Characteristics	Patients, N (%)
No. of patients	73 (100,0%)
Age, N (%)	
<65 yo (%)	33 (45,2%)
>65 yo (%)	40 (54,8%)
Sex, N (%)	
Male	52 (71,2%)
Female	21 (28,8%)
ECOG PS, N (%)	
0-1	42 (57,5%)
≥2	31 (42,5%)
Histology, N (%)	
Adenocarcinoma	56 (76,7%)
Squamous cell carcinoma	13 (17,8%)
Others	4 (5,5%)
Smoking history, N (%)	
Never	12 (16,4%)
Former/current	56 (76,7%)
NA	5 (6,9 %)
Tumor site, N (%)	
Left	35 (48,0%)
Right	30 (41,0%)
Bilateral	5 (6,9%)
NA	3 (4,1%)
Metastases distribution, N (%)	
Bone	24 (32,8%)
Nodes	62 (84,9%)
CNS	14 (19,2%)
Liver	9 (12,3%)
Adrenal gland	13 (17,8%)
Other	14 (19,2%)
Therapy, N (%)	
TKI, 19 (26.0%)	EGFR TKI, 9 (12,3%) ALK TKI, 5 (6,9%) ROS-1 TKI, 2 (2,7%) BRAF + MEK TKI, 3 (4,1%)
IO-based, 28 (38.3%)	single-agent IO, 13 (15%) IO plus CT, 15 (20,5%)
CT, 26 (35.6%)	26 (35,6%)

Table 1. Baseline patients' characteristics

Characteristics			**Patients, N (%)**	
No. of patients			73 (100,0%)	
Diagnostic techniques, N (%)				
Tissue, 73 (100%)	Real Time-PCR,	55 (75,3%)	wt, 44 (80%)	
			mutated, 11 (20%)	*EGFR* 8*, BRAF* 3
	NGS	9 (12,3%)	wt, 3 (33,3%)	
			altered, 6 (66,6%)	*EGFR* 2, *KRAS* 2, *ALK* 1, *MET* 1*, RET* 1*, ROS1* 1
	NA	13 (17,8%)	-	-
Plasma, 10 (13.6%)	Droplet Digital PCR	5 (50%)	wt, 3 (60%)	
			mutated 2 (40%)	*EGFR* 2
	NGS	5 (50%)	wt, 0 (0%)	
			altered, 5 (100%)	*EGFR* 2*, BRAF* 1, *KRAS* 1, *EGFR* + *TP53* 1
Tissue predictive biomarker testing, N (%)				
IHC	PD-L1, 67 (91,7%)	≥ 50% 1-49% <1% NA	16 (21,9%) 27 (36,9%) 24 (32,8%) 6 (8,2%)	
	ALK, 56 (76,7%)	Positive Negative NA	4 (5,4%) 52 (71,2%) 17 (23,2%)	
	ROS1, 46 (63,0%)	Positive Negative NA	3 (4,1%) – 1 confirmed by FISH (1,3%) 43 (58,9%) 27 (37,0%)	
Molecular diagnostics	*EGFR*, 9 (12,3%)		p.E746_A750del, 3 p.E746_A750del + p.T790M + p.R175H, TP53, 1 p.E746_A750del + p.C797S, 1 p.L858R, 3 p.L861Q,1	
	KRAS, 2		p.G12V, 1 p.G12D, 1	
	BRAF, 3		p.V600E, 3	
	ROS1, 1		ROS1-CD74, 1	
	ALK, 1		EML4(6)-ALK(20), 1	
	RET, 1		KIF5B – RET, 1	
	MET, 1		amplification, 1	
	NTRK1/2/3, 0		-	
	HER-2, 0		-	
Plasma predictive biomarker testing, N				
Molecular diagnostics	*EGFR*, 2		p.E746_A750del, 1 p.E746_A750del + p.T790M + p.R175H, TP53; 1	
	BRAF, 1		p.V600E, 1	
	KRAS, 1		p.G12V, 1	
Therapy, N (%)				
TKI, 19 (26.0%)			EGFR TKI, 9 (12,3%) ALK TKI, 5 (6,9%) ROS-1 TKI, 2 (2,7%) BRAF + MEK TKI, 3 (4,1%)	
IO-based, 28 (38.3%)			single-agent IO, 13 (15%) IO plus CT, 15 (20,5%)	
CT, 26 (35.6%)			26 (35,6%)	

Table 2. Diagnostic techniques performed during the conduction of the study

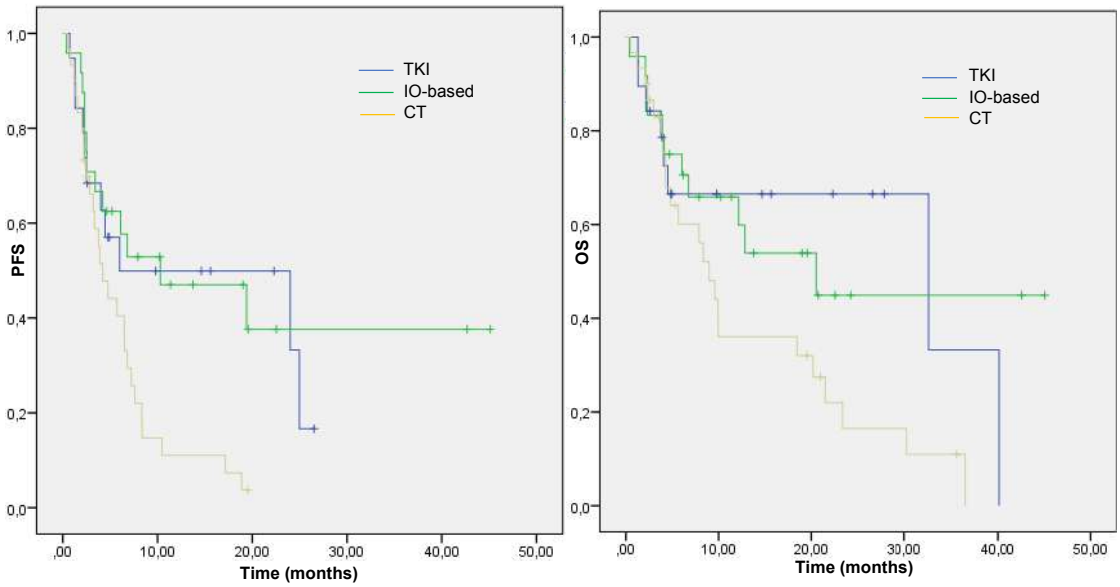

Figure 1. Kaplan–Meier analysis of PFS and OS in NSCLC patients according to treatment subgroups.

TKI, tyrosine kinase inhibitor; IO, immune-oncology; CT, platinum-based chemotherapy; NSCLC, non-small cell lung cancer; PFS, progression-free survival; OS, overall survival

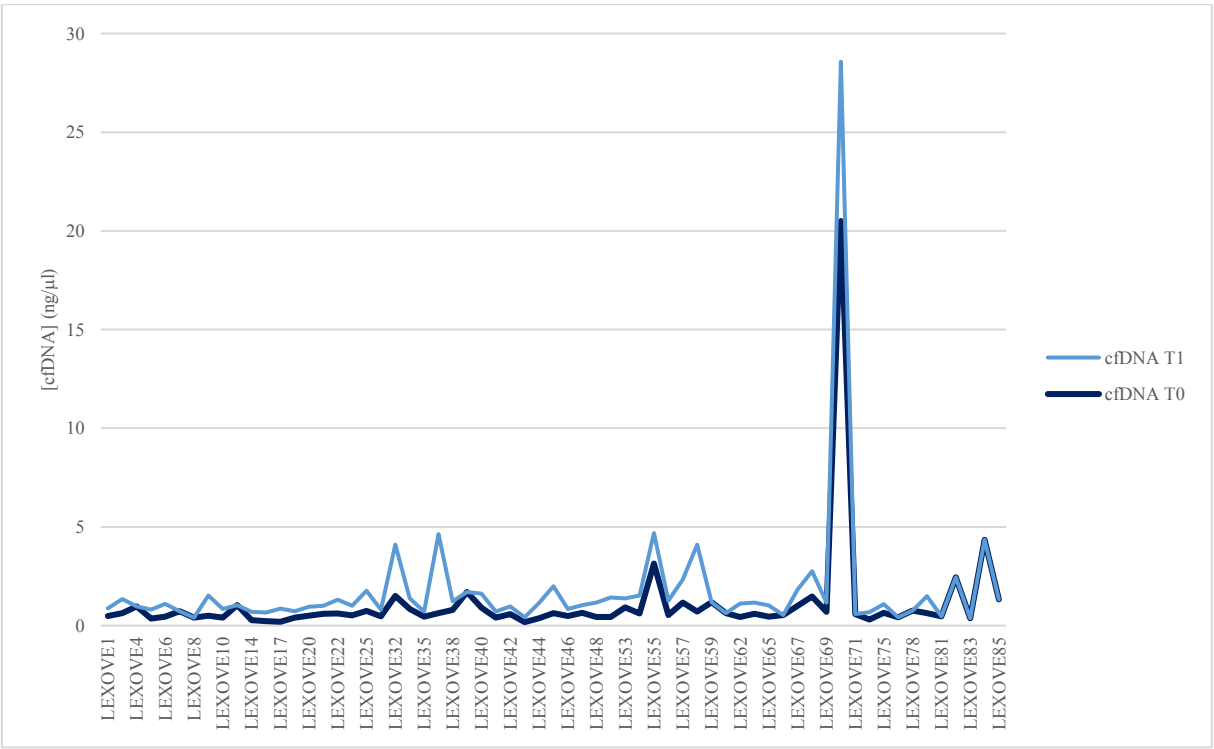

Figure 2. Graphical representation of cfDNA dynamics from baseline (T0) to the radiologic evaluation (T1).

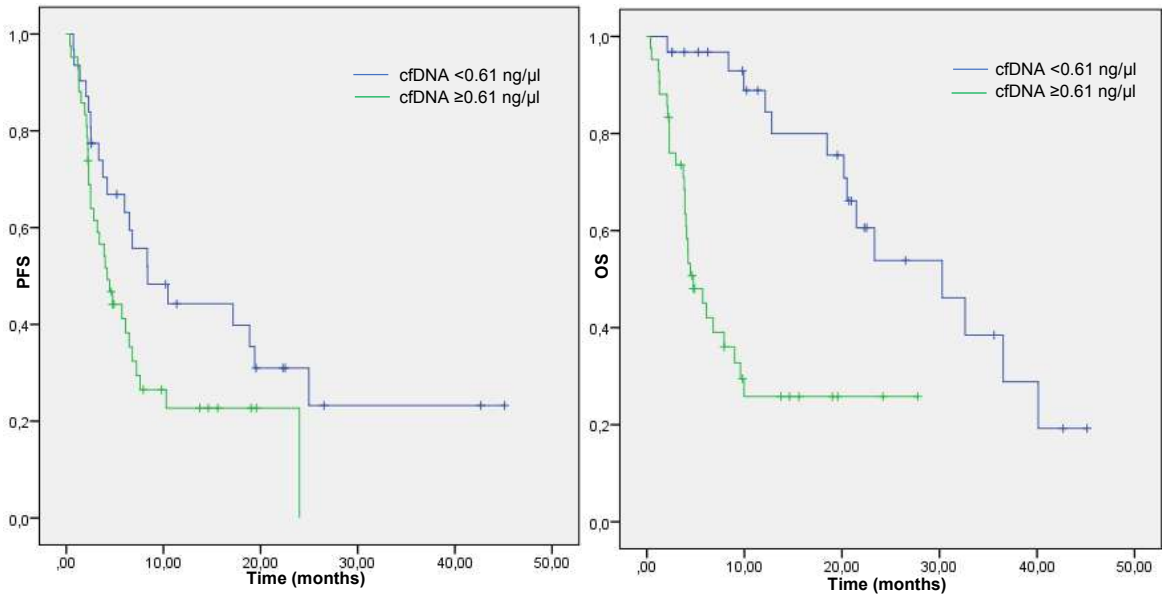

Figure 3. Kaplan–Meier analysis of PFS and OS according to the median cfDNA value in the overall cohort population.

cfDNA, cell-free DNA; PFS, progression-free survival; OS, overall survival.

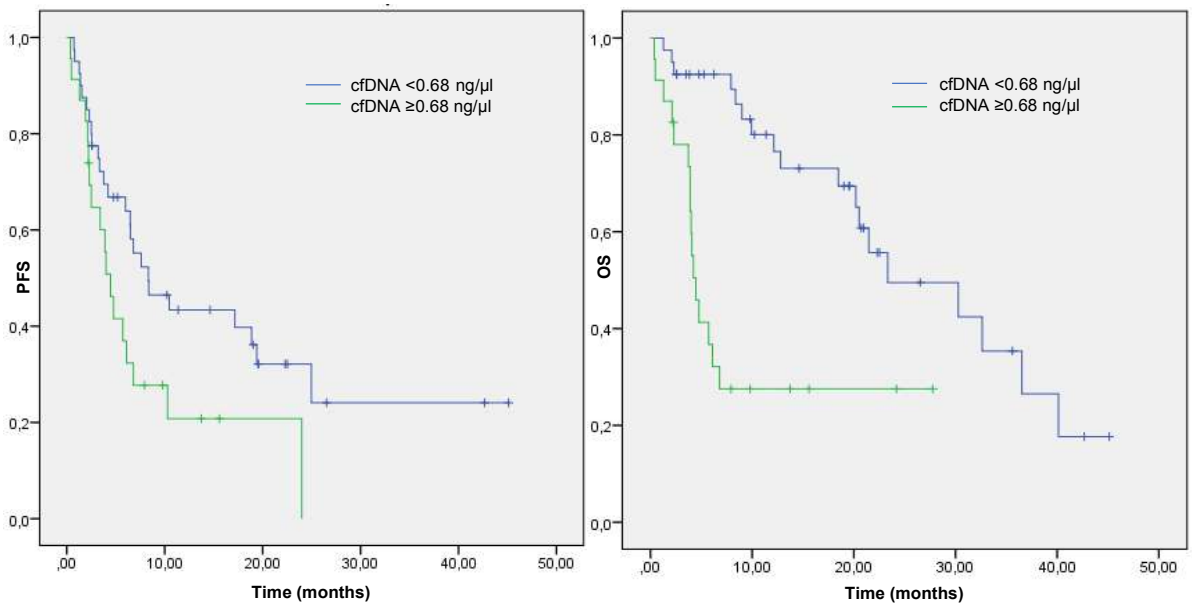

Figure 4. Kaplan–Meier analysis of PFS and OS according to the cfDNA cut-off based on X-tile analysis in the overall cohort population.

cfDNA, cell-free DNA; PFS, progression-free survival; OS, overall survival.

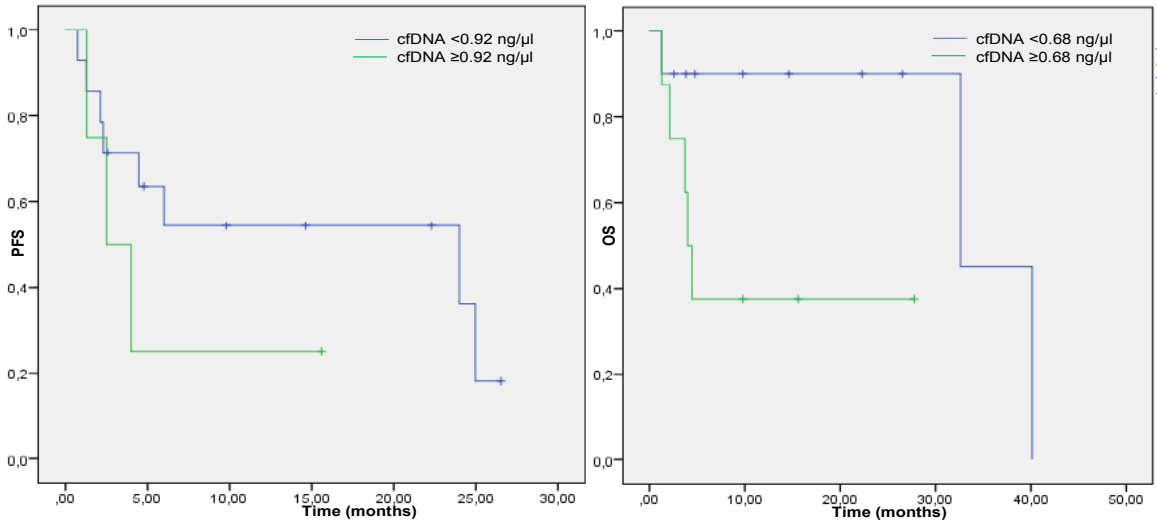

Figure 5. Kaplan–Meier analysis of PFS and OS according to the cfDNA cut-off based on X-tile analysis in patients with NSCLC receiving TKIs.

cfDNA, cell-free DNA; PFS, progression-free survival; OS, overall survival; NSCLC, non-small cell lung cancer; TKI, tyorisine kinase inhibitor

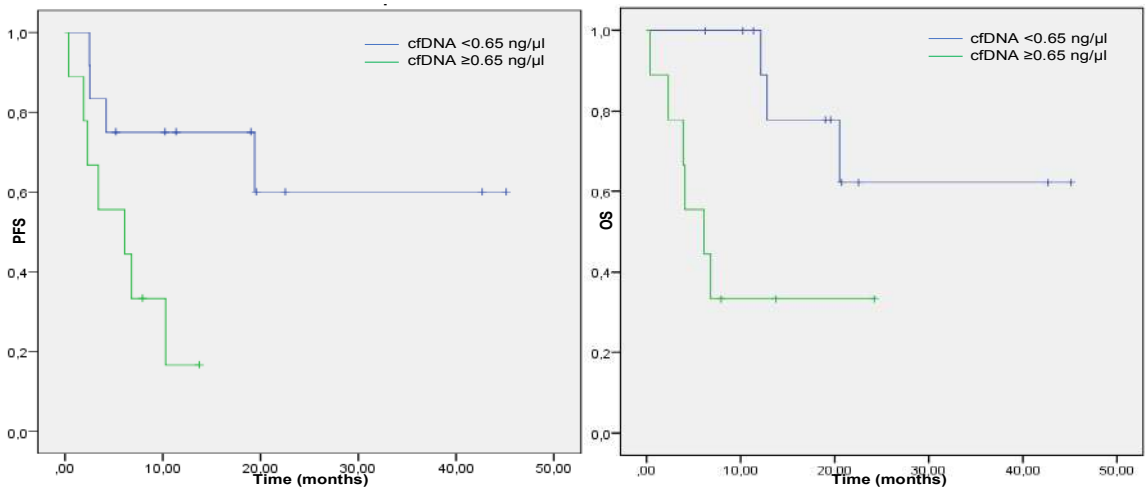

Figure 6. Kaplan–Meier analysis of PFS and OS according to the cfDNA cut-off based on X-tile analysis in patients with NSCLC receiving IO-based treatments.

cfDNA, cell-free DNA; PFS, progression-free survival; OS, overall survival; NSCLC, non-small cell lung cancer; IO, immune-oncology.

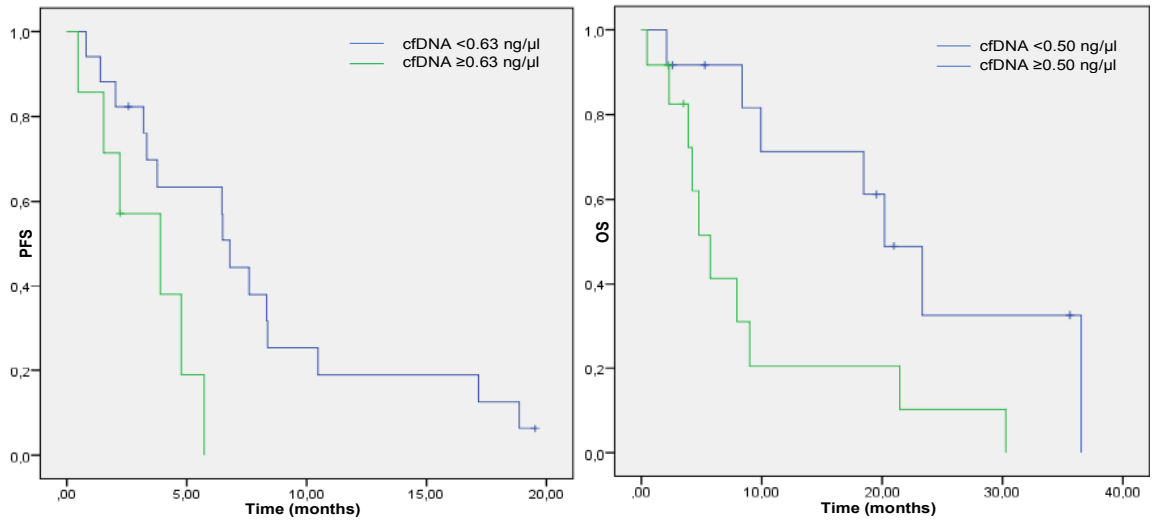

Figure 7. Kaplan–Meier analysis of PFS and OS according to the cfDNA cut-off based on X-tile analysis in patients with NSCLC receiving CT.

cfDNA, cell-free DNA; PFS, progression-free survival; OS, overall survival; NSCLC, non-small cell lung cancer; CT, platinum-based chemotherapy.

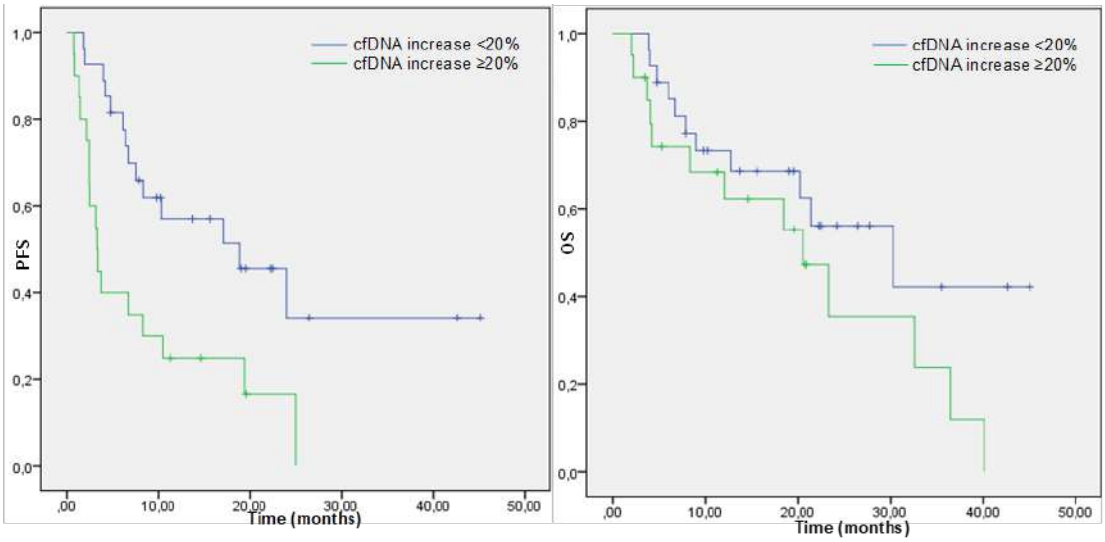

Figure 8. Kaplan–Meier analysis of PFS and OS according to the cfDNA increase at first restaging in the overall cohort population.

cfDNA, cell-free DNA; PFS, progression-free survival; OS, overall survival

	N	Events	Univariate			Multivariate	
			PFS (median months)	95% CI	p (log rank)	p	HR (95% CI)
Sex					0.088		
M	52	41	4.8	2,77-6,76			
F	21	10	17.2	1,99-32,34			
Age					0.282		
<65	33	22	6.8	1,15-12,07			
≥65	40	29	5.7	3,23-8,22			
ECOG PS					**0.029**		
0	27	16	10.3	0-22,78			
1	13	10	5.7	1,85-9,60			
2	33	25	4.2	2,33-6,06			
Smoking status					0.094		
Never	13	7	17.2	2,25-32,09			
Current/former	56	40	6.1	3,95-8,25			
Histology					0.517		
non-squamous	60	41	6.0	3,72-8,27			
squamous	13	10	6.5	2,26-10,67			
Brain metastasis					0.957		
No	59	41	6.0	3,11-8,89			
Yes	14	10	6.1	2,57-9,63			
Bone metastasis							
No	46	30	6.8	4,02-9,58			
Yes	27	21	5.7	2,7-8,76			
Liver metastasis					**<0,0001**	**<0,0001**	0,027 (0,004-0,175)
No	61	41	6.8	4,93-8,67			
Yes	10	9	1.3	0-2,63			
Adrenal metastasis					**<0,014**		
No	59	39	6.8	4,27-9,33			
Yes	14	12	2.2	0-5,33			
Site of disease					**0.248**		
Intra-thoracic	22	14	8.3	6,28-10,38			
Extra-thoracic	49	36	4.5	2,23-6,71			
Median cfDNA					**0.043**		
<0,61	31	20	8.4	2,46-14,27			
≥0,61	42	31	4.2	2,51-5,88			
cfDNA increase					**0.004**	**0.005**	0,345 (0,165-0,722)
<20%	27	14	18.9	6,25-31,48			
≥20%	20	17	3.3	2,89-3,76			

Table 3. Univariate and multivariate analysis of progression-free survival (PFS).

	N	Events	Univariate			Multivariate	
			OS (median months)	95% CI	p (log rank)	p	HR (95% CI)
Sex					0.079		
M	52	34	9.9	5,68-14,25			
F	21	8	40.1	0-85,59			
Age					0.51		
<65	33	19	21.5	15,87-27,06			
≥65	40	23	9.9	7,37-12,48			
ECOG PS					**<0,0001**		
0	27	11	36.0	28,60-43,39		**0.004**	**0,226 (0,083- 0,614)**
1	13	9	20.2	7,36-33,03		0.597	0,79 (0,330-1,890)
2	33	22	6.1	2,48-9,71			1
Smoking status					0.16		
Never	13	6	32.6	0-73,06			
Current/former	56	32	12.8	1,87-23,73			
Histology					0.715		
non-squamous	60	35	10.0	0-25,48			
squamous	13	7	18.5	1,9-35,03			
Brain metastasis					0.22		
No	46	23	20.5	6,85-34,2			
Yes	27	19	9.0	3,14-14,8			
Bone metastasis					0.063		
No	46	23	20.5	6,85-34,2			
Yes	27	19	9.0	3,14-14,85			
Liver metastasis					**0.012**	**0.004**	0,314 (0,141-0,697)
No	61	33	18.5	6,95-29,98			
Yes	10	9	2.1	0-4,71			
Adrenal metastasis					**<0,0001**		
No	59	31	20.5	10,96-30,10			
Yes	14	11	3.9	2,01-5,78			
Site of disease					**0.017**		
Intra-thoracic	22	10	30.3	16,45-44,08			
Extra-thoracic	49	32	9.6	3,35-15,84			
Median cfDNA					**<0,0001**	**0.001**	0,212 (0,088-0,510)
<0,61	31	14	30.3	18,38-42,15			
≥0,61	42	28	4.8	2,48-7,05			
cfDNA increase					0.129		
<20%	27	11	30.3	12,21-48,32			
≥20%	20	13	20.5	14,44-26,62			

Table 4. Univariate and multivariate analysis overall survival (OS).

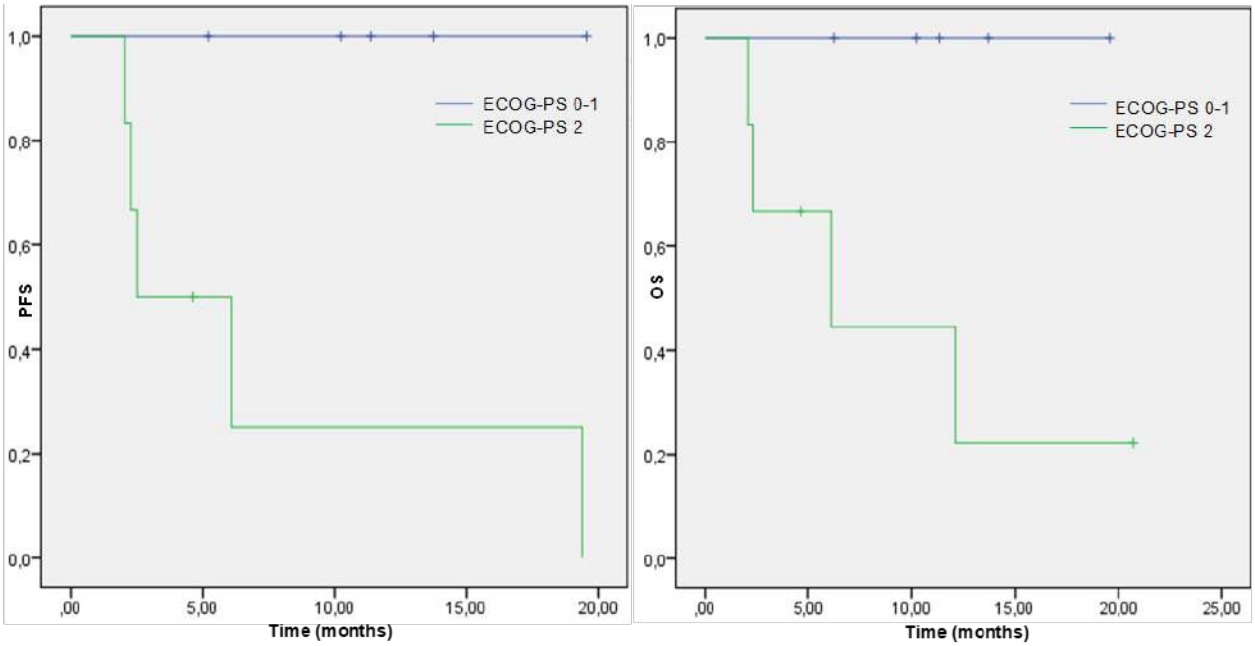

Figure 9. Kaplan–Meier analysis of PFS and OS according to ECOG-PS in patients with NSCLC receiving CT plus IO.

PFS, progression-free survival; OS, overall survival; ECOG-PS, Eastern Cooperative Oncology Group Performance Status; NSCLC, non-small cell lung cancer; CT, platinum-based chemotherapy; IO, immune-oncology.

ID	Therapy	SCAN	cfDNA/cfEXO		R90		DZ		PDI	
			T0	T1	T0	T1	T0	T1	T0	T1
HEALTHY	-	-	0.33/NA	0.32/NA	815 ± 8	694 ± 7	284 ± 5	290 ± 10	0,25 ± 0.01	0,23 ± 0.01
LEXOVE 5	CT	SD	0.36/NA	NA/1.28	3150 ± 125	2100 ± 105	204 ± 5	252 ± 10	0.25 ± 0.01	0.09 ± 0.01
LEXOVE 11	CT	PD	1.04/2.35	NA/NA	2210 ± 150	NA	234 ± 15	NA	0.20 ± 0.01	NA
LEXOVE 14	EGFR TKI	PD	0.42/NA	0.72/1.12	1650 ± 95	1770 ± 75	240 ± 10	234 ±10	0.15 ± 0.01	0.17 ± 0.01
LEXOVE 16	ALK TKI	PD	0.23/NA	0.48/1.94	2830 ± 100	3240 ± 110	222 ± 5	228 ± 5	0.17 ± 0.01	0.14 ± 0.01
LEXOVE 17	CT	SD	0.20/1.34	0.66/1.66	3120 ± 100	2900 ± 75	240 ± 10	222 ± 5	0.12 ± 0.01	0.10 ± 0.01
LEXOVE 20	CT	SD	0.50/1.58	NA/NA	1980 ± 70	3050 ± 80	240 ±10	216 ±5	0.16 ± 0.01	0.23 ± 0.01
LEXOVE 32	ALK TKI	PD	1.50/1.60	2.60/2.06	2870 ± 100	1980 ± 90	246 ± 10	246 ±10	0.15 ± 0.01	0.14 ± 0.01
LEXOVE 33	EGFR TKI	PR	0.84/0.96	0.54/1.18	3210 ± 30	NA	260 ± 5	NA	0,14 ± 0.01	NA
LEXOVE 35	EGFR TKI	PR	0.45/NA	0.27/1.8	2510 ± 80	1590 ± 100	216 ± 5	234 ± 10	0.15 ± 0.01	0.17 ± 0.01
LEXOVE 36	IO	PD	0.69/NA	NA/NA	376 ± 150	NA	222 ±10	NA	0.17 ± 0.01	NA
LEXOVE 38	IO	PR	0.79/1.92	0.44/0.96	2030 ± 20	4190 ± 40	260 ± 5	250 ± 5	0.32 ± 0.01	0.22 ± 0.01
LEXOVE 41	IO	PR	0.40/1.22	0.31/1.12	1758 ± 18	1802 ± 18	219 ± 15	235 ± 7	0.27 ± 0.01	0.19 ± 0.01
LEXOVE 42	EGFR TKI	PR	0.59/1.76	0.38/1.78	2510 ± 100	1280 ± 60	240 ±10	240 ± 10	0.22 ± 0.01	0.12 ± 0.01
LEXOVE 47	IO	PR	0.65/1.4	0.39/1.02	6740 ± 70	1890 ± 19	183 ± 5	232 ± 5	0.29 ± 0.01	0.22 ± 0.01
LEXOVE 53	EGFR TKI	PR	0.92/1.08	0.46/1.14	1478 ± 15	1330 ± 14	241 ± 5	256 ± 5	0.29 ± 0.01	0.22 ± 0.01
LEXOVE 65	EGFR TKI	PR	0.45/0.80	0.51/1.06	5630 ± 60	2980 ± 30	189 ± 5	182 ± 10	0,40 ± 0.01	0,32 ± 0.01
LEXOVE 67	IO	PR	1.01/2.38	0.83/2.08	NA	NA	NA	NA	NA	NA
LEXOVE 68	CT+IO	PR	1.47/2.22	1.29/2.18	NA	NA	NA	NA	NA	NA
LEXOVE 69	IO	PR	0.7/1.56	0.47/2.32	NA	NA	NA	NA	NA	NA
LEXOVE 70	ALK TKI	PR	8.07/1.22	20/NA	NA	NA	NA	NA	NA	NA
LEXOVE 71	CT+IO	PR	0.58/1.66	NA/NA	NA	NA	NA	NA	NA	NA
LEXOVE 73	CT+IO	PD	0.30/1.22	0.38/2.06	NA	NA	NA	NA	NA	NA

Table 5. Extracellular vesicles (EVs) characterization evaluating R90, Dz and PDI levels among 22 patients with advanced non-small cell lung cancer and healthy donor as compared to cell-free DNA (cfDNA) and EVS protein content (cfEXO) at baseline (T0) and at the time of radiologic response.

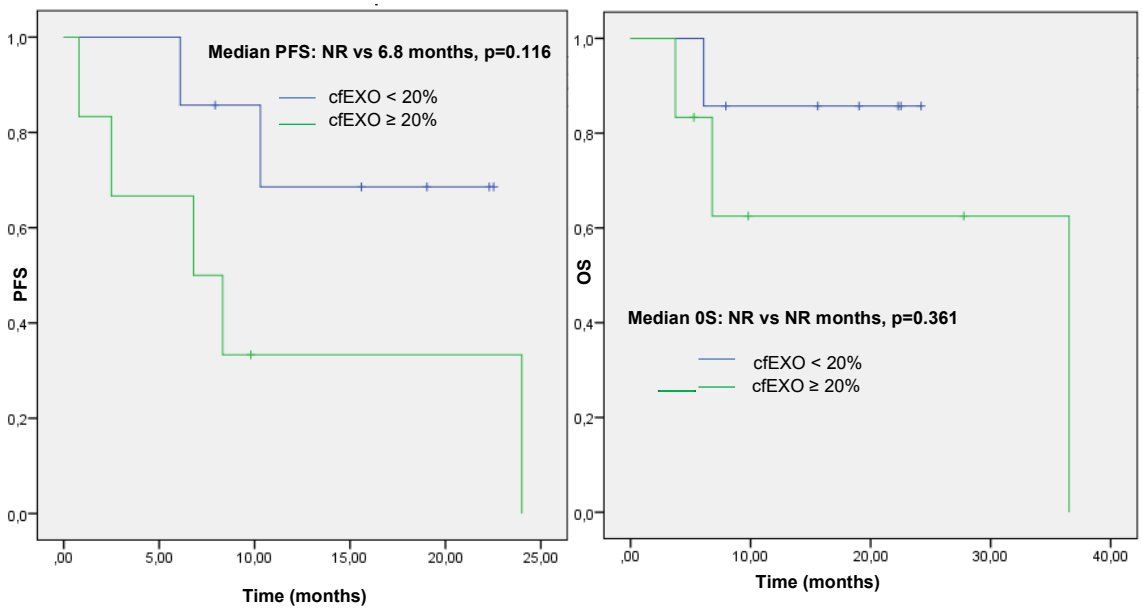

Figure 10. Kaplan–Meier analysis of PFS and OS in NSCLC patients according to cfEXO.

cfEXO, circulating-free extracellular vesicle protein concentration; NSCLC, non-small cell lung cancer; PFS, progression-free survival; OS, overall survival

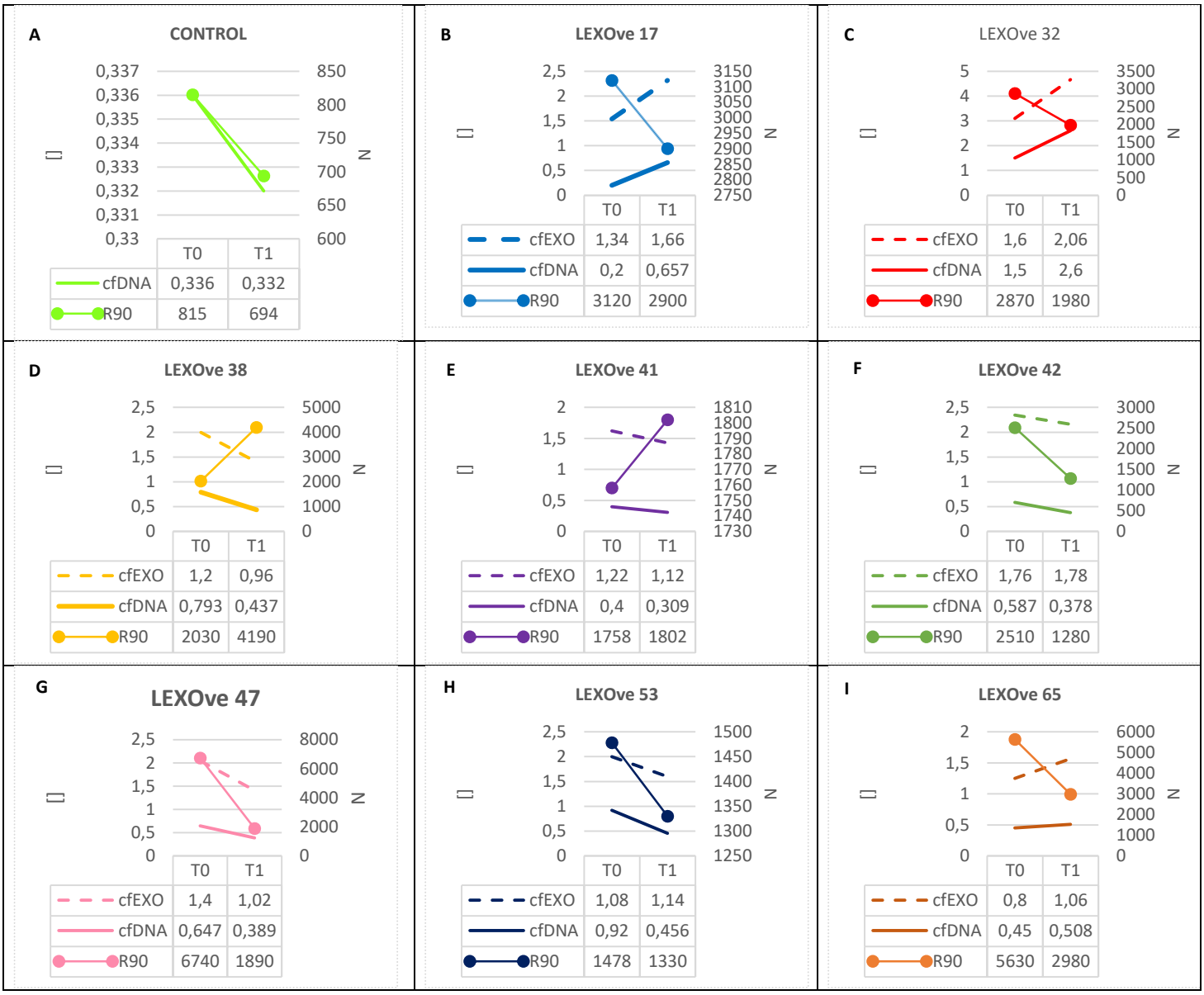

Figure 11. Real time longitudinally monitoring of treatment-naïve patients using cell-free DNA, extracellular vesicles (EVs) protein content (cfEXO) and R90 levels as compared to healthy control at baseline (T0) and at the time of radiologic evaluation (T1).

References

1. Siegel, R. L., Miller, K. D. & Jemal, A. Cancer statistics, 2020. *CA. Cancer J. Clin.* (2020) doi:10.3322/caac.21590.
2. Siegel, R. L., Miller, K. D., Fuchs, H. E. & Jemal, A. Cancer statistics, 2022. *CA. Cancer J. Clin.* (2022) doi:10.3322/caac.21708.
3. Passiglia, F. *et al.* Lung Cancer in Italy. *Journal of Thoracic Oncology* (2019) doi:10.1016/j.jtho.2019.05.019.
4. Costa, D. B. & Kobayashi, S. S. Whacking a mole-cule: Clinical activity and mechanisms of resistance to third generation EGFR inhibitors in EGFR mutated lung cancers with EGFR-T790M. *Translational Lung Cancer Research* (2015) doi:10.3978/j.issn.2218-6751.2015.05.05.
5. Soria, J.-C. *et al.* Osimertinib in Untreated EGFR -Mutated Advanced Non–Small-Cell Lung Cancer . *N. Engl. J. Med.* (2018) doi:10.1056/nejmoa1713137.
6. Stewart, E. L., Tan, S. Z., Liu, G. & Tsao, M. S. Known and putative mechanisms of resistance to EGFR targeted therapies in NSCLC patients with EGFR mutations-a review. *Translational Lung Cancer Research* (2015) doi:10.3978/j.issn.2218-6751.2014.11.06.
7. Mao, C. *et al.* Blood as a Substitute for Tumor Tissue in Detecting EGFR Mutations for Guiding EGFR TKIs Treatment of Nonsmall Cell Lung Cancer. *Medicine (United States)* (2015) doi:10.1097/MD.0000000000000775.
8. Shroff, G. S., de Groot, P. M., Papadimitrakopoulou, V. A., Truong, M. T. & Carter, B. W. Targeted Therapy and Immunotherapy in the Treatment of Non–Small Cell Lung Cancer. *Radiologic Clinics of North America* (2018) doi:10.1016/j.rcl.2018.01.012.
9. Russo, A. *et al.* The molecular profiling of solid tumors by liquid biopsy: a position paper of the AIOM–SIAPEC-IAP–SIBioC–SIC–SIF Italian Scientific Societies. *ESMO Open* (2021) doi:10.1016/j.esmoop.2021.100164.
10. Zhou, X. *et al.* Kinetics of plasma cfDNA predicts clinical response in non-small cell lung cancer patients. *Sci. Rep.* (2021) doi:10.1038/s41598-021-85797-z.
11. Dietz, S. *et al.* Longitudinal therapy monitoring of ALK-positive lung cancer by combined copy number and targeted mutation profiling of cell-free DNA. *EBioMedicine* (2020) doi:10.1016/j.ebiom.2020.103103.
12. Xavier, C. P. R. *et al.* The Role of Extracellular Vesicles in the Hallmarks of Cancer and Drug Resistance. *Cells* (2020) doi:10.3390/cells9051141.
13. Galvano, A. *et al.* The prognostic impact of tumor mutational burden (TMB) in the first-line management of advanced non-oncogene addicted non-small-cell lung cancer (NSCLC): a systematic review and meta-analysis of randomized controlled trials. *ESMO Open* (2021) doi:10.1016/j.esmoop.2021.100124.
14. Gristina, V. *et al.* The emerging therapeutic landscape of alk inhibitors in non-small cell lung cancer. *Pharmaceuticals* (2020) doi:10.3390/ph13120474.
15. Galvano, A. *et al.* Analysis of systemic inflammatory biomarkers in neuroendocrine carcinomas of the lung: prognostic and predictive significance of NLR, LDH, ALI, and LIPI score. *Ther. Adv. Med. Oncol.* (2020) doi:10.1177/1758835920942378.

16. Passiglia, F. *et al.* Is there any place for PD-1/CTLA-4 inhibitors combination in the first-line treatment of advanced NSCLC?—a trial-level meta-analysis in PD-L1 selected subgroups. *Translational Lung Cancer Research* (2021) doi:10.21037/tlcr-21-52.
17. Silva, J. *et al.* Analysis of exosome release and its prognostic value in human colorectal cancer. *Genes Chromosom. Cancer* (2012) doi:10.1002/gcc.21926.
18. Duijvesz, D. *et al.* Immuno-based detection of extracellular vesicles in urine as diagnostic marker for prostate cancer. *Int. J. Cancer* (2015) doi:10.1002/ijc.29664.
19. Skog, J. *et al.* Glioblastoma microvesicles transport RNA and proteins that promote tumour growth and provide diagnostic biomarkers. *Nat. Cell Biol.* (2008) doi:10.1038/ncb1800.
20. Li, P. & Qin, C. Elevated circulating VE-cadherin + CD144 + endothelial microparticles in ischemic cerebrovascular disease. *Thromb. Res.* (2015) doi:10.1016/j.thromres.2014.12.006.
21. Liu, C., Yang, Y. & Wu, Y. Recent Advances in Exosomal Protein Detection Via Liquid Biopsy Biosensors for Cancer Screening, Diagnosis, and Prognosis. *AAPS Journal* (2018) doi:10.1208/s12248-018-0201-1.
22. Serrano-Pertierra, E. *et al.* Characterization of plasma-derived extracellular vesicles isolated by different methods: A comparison study. *Bioengineering* (2019) doi:10.3390/bioengineering6010008.
23. Ng, C., Pircher, A., Augustin, F. & Kocher, F. Evidence-based follow-up in lung cancer? *memo - Mag. Eur. Med. Oncol.* (2020) doi:10.1007/s12254-020-00575-3.
24. Incorvaia, L. *et al.* Programmed Death Ligand 1 (PD-L1) as a Predictive Biomarker for Pembrolizumab Therapy in Patients with Advanced Non-Small-Cell Lung Cancer (NSCLC). *Advances in Therapy* (2019) doi:10.1007/s12325-019-01057-7.
25. Kato, H., Nakamura, A., Takahashi, K. & Kinugasa, S. Accurate size and size-distribution determination of polystyrene latex nanoparticles in aqueous medium using dynamic light scattering and asymmetrical flow field flow fractionation with multi-angle light scattering. *Nanomaterials* (2012) doi:10.3390/nano2010015.
26. Romancino, D. P. *et al.* Palmitoylation is a post-translational modification of Alix regulating the membrane organization of exosome-like small extracellular vesicles. *Biochim. Biophys. Acta - Gen. Subj.* (2018) doi:10.1016/j.bbagen.2018.09.004.
27. Adamo, G. *et al.* Nanoalgosomes: Introducing extracellular vesicles produced by microalgae. *J. Extracell. Vesicles* (2021) doi:10.1002/jev2.12081.
28. Schmitz, K. S. & Phillies, G. D. J. An Introduction to Dynamic Light Scattering by Macromolecules . *Phys. Today* (1991) doi:10.1063/1.2810116.
29. Ignatiadis, M., Sledge, G. W. & Jeffrey, S. S. Liquid biopsy enters the clinic — implementation issues and future challenges. *Nature Reviews Clinical Oncology* (2021) doi:10.1038/s41571-020-00457-x.
30. Aggarwal, C. *et al.* Baseline Plasma Tumor Mutation Burden Predicts Response to Pembrolizumab-based Therapy in Patients with Metastatic Non–Small Cell Lung Cancer. *Clin. Cancer Res.* (2020) doi:10.1158/1078-0432.CCR-19-3663.
31. Garassino, M. C. *et al.* Evaluation of blood TMB (bTMB) in KEYNOTE-189: Pembrolizumab (pembro) plus chemotherapy (chemo) with pemetrexed and platinum versus placebo plus chemo as first-line therapy for metastatic nonsquamous NSCLC. *J. Clin. Oncol.* (2020) doi:10.1200/jco.2020.38.15_suppl.9521.
32. Zhang, Q. *et al.* Prognostic and predictive impact of circulating tumor dna in patients with advanced cancers treated with immune checkpoint blockade. *Cancer Discov.* (2020) doi:10.1158/2159-8290.CD-20-0047.
33. Anagnostou, V. *et al.* Dynamics of tumor and immune responses during immune checkpoint blockade in non–small cell lung cancer. *Cancer Res.* (2019) doi:10.1158/0008-5472.CAN-18-1127.
34. Gandhi, L. *et al.* Pembrolizumab plus Chemotherapy in Metastatic Non–Small-Cell Lung

Cancer. *N. Engl. J. Med.* (2018) doi:10.1056/nejmoa1801005.
35. Reck, M. *et al.* Pembrolizumab versus Chemotherapy for PD-L1–Positive Non–Small-Cell Lung Cancer. *N. Engl. J. Med.* (2016) doi:10.1056/nejmoa1606774.
36. Gridelli, C. *et al.* First-line immunotherapy in advanced non-small-cell lung cancer patients with ECOG performance status 2: results of an International Expert Panel Meeting by the Italian Association of Thoracic Oncology. *ESMO Open* (2022) doi:10.1016/j.esmoop.2021.100355.
37. Hyun, M. H. *et al.* Quantification of circulating cell-free DNA to predict patient survival in non-small-cell lung cancer. *Oncotarget* (2017) doi:10.18632/oncotarget.21769.
38. Waterhouse, D. *et al.* Real-world outcomes of immunotherapy–based regimens in first-line advanced non-small cell lung cancer. *Lung Cancer* (2021) doi:10.1016/j.lungcan.2021.04.007.
39. Dall'Olio, F. G. *et al.* ECOG performance status ≥2 as a prognostic factor in patients with advanced non small cell lung cancer treated with immune checkpoint inhibitors—A systematic review and meta-analysis of real world data. *Lung Cancer* (2020) doi:10.1016/j.lungcan.2020.04.027.

Scientific Products (during the Ph.D. course)

In extenso:

- The Diagnostic Accuracy of PIK3CA Mutations by circulating tumor DNA (ctDNA) in Breast Cancer: An Individual Patient Data Meta-analysis.
  Therapeutic Advances in Medical Oncology. IN PRESS
  10.1177/17588359221110162

- Extracellular Vesicles-ceRNAs as Ovarian Cancer Biomarkers: Looking into circRNA-miRNA-mRNA Code.
  Cancers (Basel). 2022 Jul 13;14(14):3404. doi: 10.3390/cancers14143404.

- TargetPlex FFPE-Direct DNA Library Preparation Kit for SiRe NGS panel: An international performance evaluation study
  Journal of Clinical Pathology, 2022, 75(6), pp. 416–421

- Safety and effectiveness of gemcitabine for the treatment of classic Kaposi's sarcoma without visceral involvement.
  Therapeutic Advances in Medical Oncology, 2022, 14

- Next generation diagnostic algorithm in non-small cell lung cancer predictive molecular pathology: The KWAY Italian multicenter cost evaluation study
  Critical Reviews in Oncology/Hematology, 2022, 169, 103525

- A narrative review on the implementation of liquid biopsy as a diagnostic tool in thoracic tumors during the COVID-19 pandemic
  Mediastinum, 2021, 5, 27

- Is there any place for PD-1/CTLA-4 inhibitors combination in the first-line treatment of advanced NSCLC? a trial-level meta-analysis in PD-L1 selected subgroups
  Translational Lung Cancer Research, 2021, 10(7), pp. 3106–3119

- The molecular profiling of solid tumors by liquid biopsy: a position paper of the AIOM–SIAPEC-IAP–SIBioC–SIC–SIF Italian Scientific Societies
  ESMO Open, 2021, 6(3), 100164

- The prognostic impact of tumor mutational burden (TMB) in the first-line management of advanced non-oncogene addicted non-small-cell lung cancer (NSCLC): a systematic review and meta-analysis of randomized controlled trials
  ESMO Open, 2021, 6(3), 100124

- Tumor mutational burden on cytological samples: A pilot study
  Cancer Cytopathology, 2021, 129(6), pp. 460–467

- Is there any room for PD-1 inhibitors in combination with platinum-based chemotherapy as frontline treatment of extensive-stage small cell lung cancer? A systematic review and

meta-analysis with indirect comparisons among subgroups and landmark survival analyses. Therapeutic Advances in Medical Oncology, 2021, 13

- KRAS mutations testing in non-small cell lung cancer: The role of Liquid biopsy in the basal setting
  Journal of Thoracic Disease, 2020, 12(7), pp. 3836–3843

- The significance of epidermal growth factor receptor uncommon mutations in non-small cell lung cancer: A systematic review and critical appraisal
  Cancer Treatment Reviews, 2020, 85, 101994

- Moving the target on the optimal adjuvant strategy for resected pancreatic cancers: A systematic review with meta-analysis.
  Cancers, 2020, 12(3), 534

- The emerging therapeutic landscape of alk inhibitors in non-small cell lung cancer
  Pharmaceuticals, 2020, 13(12), pp. 1–23, 474

- Analysis of systemic inflammatory biomarkers in neuroendocrine carcinomas of the lung: prognostic and predictive significance of NLR, LDH, ALI, and LIPI score
  Therapeutic Advances in Medical Oncology, 2020, 12

- Programmed Death Ligand 1 (PD-L1) as a Predictive Biomarker for Pembrolizumab Therapy in Patients with Advanced Non-Small-Cell Lung Cancer (NSCLC)
  Advances in Therapy, 2019, 36(10), pp. 2600–2617

Recommendations, Position papers and Guidelines (as main expert author)

- Raccomandazioni AIOM 2020 per l'esecuzione di Test Molecolari su Biopsia Liquida in Oncologia
- Raccomandazioni AIOM 2020 per l'implementazione dell'analisi mutazionale BRCA nei pazienti con adenocarcinoma del pancreas metastatico
- Linee Guida AIOM 2021 Cardioncologia

Book chapters:

UNIPA SPRINGER SERIES, Antonio Russo et al. (Eds): Practical Medical Oncology Textbook

- Thyroid cancer
- Liquid biopsy
- Gastric cancer. Locoregional disease
- Metastatic colon cancer
- Lung cancer
- Biomarkers
- Hereditary cancers and genetics